ASANSOL ENGINEERING COLLEGE
ESTD 1998

ELECTROSPARK

VOLUME – 6, ISSUE – 1, 2022-2023

DEPARTMENT OF ELECTRONICS & COMMUNICATION ENGINEERING

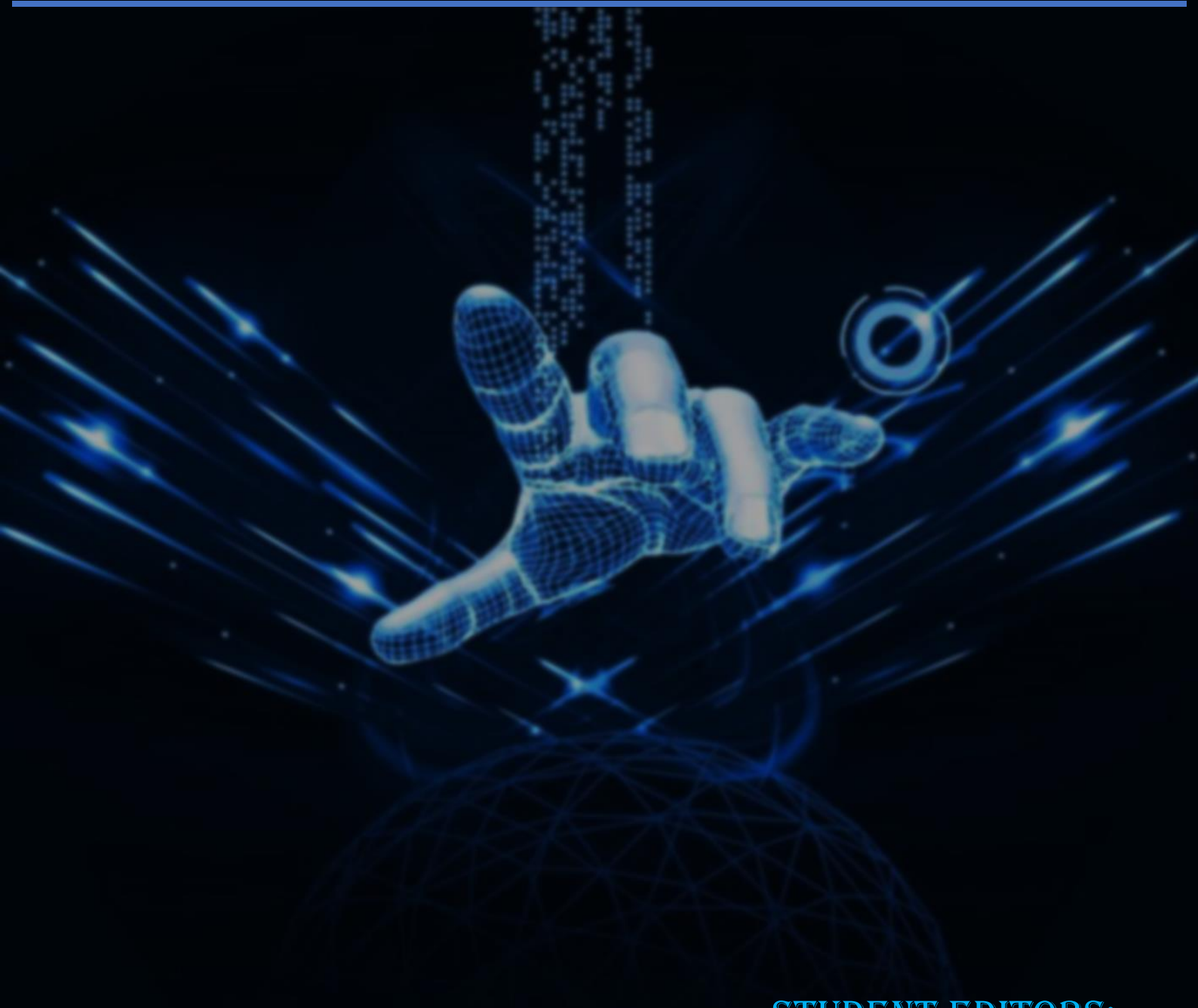

FACULTY COORDINATORS:

Mr. Sumanta Karmakar
Dr. Ashmi Chakrabory
Dr. Saswata Chakraborty
Mr. Prajit Paul

STUDENT EDITORS:

Mr. Shibram Paramanik
Ms. Anushka Trivedi
Mr. Somnil Neogi
Mr. Prince Kumar
Mr. Kaustav Biswas
Mr. Subhankar Roy
Mr. Nilanjan Dutta
Ms. Ananya Ghosh

INSTITUTE'S VISION

To emerge as a centre of excellence in technical education, offering best of the teaching and learning by creating ambience for advanced level of education and research to serve the society.

DEPARTMENT'S VISION

To aspire to become a department which can provide value-based quality education, foster research and innovation and to groom the students to be globally competent.

INSTITUTE'S MISSION

IM-1: To create an ambience for advanced level of teaching and learning process.

IM-2: To generate new ideas by engaging in cutting-edge research and technology.

IM-3: To initiate collaborative projects which offer opportunities for long term interaction with industry and academia.

IM-4: To develop intellectual human potential for serving the society according to the regional, national and global needs.

DEPARTMENT'S MISSION

DM-1: To Create an outcome-based teaching learning process to increase the creativity and innovativeness of the students and to face the challenging world.

DM-2: To motivate students and promote research and development culture among students, so that they can choose it as an optional career.

DM-3: To provide ethical and value-based education by promoting activities addressing the societal needs Editorial board.

MESSAGE FROM HOD, ECE

Dr. Chittajit Sarkar

HEAD OF DEPARTMENT
ELECTRONICS & COMMUNICATION ENGINEERING

Welcome to the department of Electronics and Communication Engineering, Asansol Engineering College. Our institution boasts a robust undergraduate program in Electronics & Communication Engineering, granting B. Tech degrees. Additionally, we provide opportunities for postgraduate studies through our M. Tech program. Each year, we admit 120 students into our B. Tech program and 13 students into the M. Tech program.

Every child possesses innate genius, and if a child isn't grasping knowledge through conventional teaching methods, perhaps it's time we adapt our approach to match their unique learning style. With this principle in mind, we've developed our teaching methodology. Our objective is to offer an outstanding platform for aspiring hardware and software engineers, equipping them to meet the ever-evolving demands of the modern industry. Our department takes pride in its commitment to academic excellence, innovation, and fostering a dynamic learning environment. As the Head of the Department, I am honored to lead a community of dedicated faculty and enthusiastic students who share a passion for knowledge and growth. Here at Electronics and Communication Engineering, we strive to provide a comprehensive educational experience that combines rigorous academic programs with practical applications. Our faculty members are not only experts in their respective fields but also mentors who are deeply invested in students' success. They are committed to nurturing students' intellectual curiosity and helping them to achieve academic and career goals.

Undergraduate students are actively encouraged to engage in a wide range of research initiatives through the Students Innovation Centre (SIC). The creation of an IEEE student chapter focused on Microwave Theory and Technology – Society further promotes and supports students in their pursuits within this field.

EDITORS' MESSAGE

It gives us immense pleasure to present to you the latest edition of our Electronics and Communication Engineering Department magazine, ELECTROSPARK. This magazine is a humble attempt to showcase the vibrant spirit, creativity, and technical brilliance of our students and faculty.

In an era where technology is evolving at an unprecedented pace, the field of Electronics and Communication remains at the heart of innovation. From the advancement of communication systems to the development of embedded technologies, our department continues to make remarkable strides in both academics and research.

This edition features a blend of technical articles and creative expressions. Each contribution reflects the passion, dedication, and intellectual curiosity of our community.

We extend our heartfelt thanks to all the students, faculty members, and contributors who have made this magazine possible. Special appreciation goes to the editorial team for their unwavering commitment and teamwork. We hope you find this edition informative, inspiring, and reflective of the dynamic world of ECE.

Warm Regards,
Shibram Paramanik, Anushka Trivedi, Somnil Neogi, Prince Kumar, Kaustav Biswas, Subhankar Roy, Nilanjan Dutta, Ananya Ghosh
Editors, ELECTROSPARK
Department of Electronics & Communication Engineering
Asansol Engineering College

INTEL'S GOAL TO BOOST 'AI EVERYWHERE' INTO THE AUTOMOTIVE INDUSTRY

KAUSTAV BISWAS, ANIMESH KUMAR SHAW
3rd YEAR, ECE

Artificial intelligence (AI) has become a crucial game-changer, advancing rapidly each day across various industries. When it comes to the automobile sector, Intel is one company taking the lead in transforming the driving experience with AI innovations. They announced at CES 2024, to acquire Silicon Mobility, a key player in the world of fabless silicon and software dedicated to deploying intelligent electric vehicle (EV) energy management solutions. This acquisition marks Intel's expansion beyond high-performance computing, as Silicon Mobility brings expertise in designing, developing, and deploying EV energy management System-on-Chips (SoCs).

Zeekr leads the way as the first to adopt AI-enhanced software-defined vehicle system-on-chips (SoCs). Andy An, President of Geely Holding Group and CEO of Zeekr Company Limited, expressed excitement about the possibilities. The forward compatibility on Intel systems combined with AI acceleration will empower Zeekr to continually scale and upgrade services, delivering next-gen experiences that customers demand. The collaboration between Intel and Zeekr exemplifies the transformative potential of AI in the automotive industry. From personalized voice assistants to adaptive driving experiences, the partnership sets the stage for a future where vehicles become intelligent companions, integrating technology into every aspect of our lives, hence the term "AI Everywhere."

The main goal is to integrate generative AI-driven living room experiences into next-gen vehicles. Jack Weast, Vice President and General Manager of Intel Automotive, highlights the significance, stating, "Intel is taking a 'whole vehicle' approach to tackle industry challenges. Applying innovative AI solutions across the vehicle platform is key for navigating the shift to EVs." He also went on to say, "This move not only aligns with Intel's sustainability goals but also addresses a critical energy management need in the automotive industry."

AI-Enhanced Software-Defined Vehicle System-on-Chips on EVs

With Intel's recent announcement at CES, Las Vegas, they emphasized on their groundbreaking AI-powered chips for cars, a fusion of Intel's AI capabilities, and a commitment to software-defined vehicles (SDVs). These SoCs promise a new frontier for in-vehicle AI applications, covering everything from monitoring drivers to creating immersive experiences inside the car.

Beyond just AI, Intel's entry into the automotive world is a strategic move to support the industry's transition to electric vehicles. To fuel a faster and smoother transition to EVs, Intel is also collaborating with SAE International to establish an automotive standard for Vehicle Platform Power Management (J3311). Inspired by proven power management techniques from the PC industry's ACPI standard, this new SAE standard aims to accelerate progress by adopting and enhancing advanced power management concepts. The goal is to make all EVs more energy-efficient and sustainable, setting a foundation for industry-wide innovation.

Moreover, they have also dedicated themselves to delivering the first open UCIe-based chiplet platform for Software-Defined Vehicles (SDVs). To successfully achieve these goals, they have also partnered with Imec, who ensure that packaging technologies meet the high quality and reliability standards of the automotive industry. With over 50 million vehicles already powered by Intel's SoCs for functions like infotainment, the vision for tomorrow includes a complete vehicle canvas for intelligent, scalable, and sustainable solutions.

Intel's vision extends beyond individual components; it's about creating a more sustainable electrified future. The integration of intelligent and programmable power devices into the automotive ecosystem is a step toward achieving this vision. The acquisition of Silicon Mobility is subject to necessary approvals, but the strategic alignment suggests a promising future for both companies.

Intel's Commitment to Open Platforms

One of the defining features of Intel's strategy is a commitment to open platforms shortly. The new family of AI-enhanced SDV SoCs is designed to address a critical industry need for power and performance scalability. These SoCs combine AI acceleration capabilities from Intel's AI PC roadmap, enabling a range of in-vehicle AI use cases, including driver and passenger monitoring.

A demonstration showcased the versatility of these SoCs, running 12 advanced workloads concurrently. From generative AI and e-mirrors to high-definition video conference calling and PC games, the SoCs exhibited their capacity to consolidate legacy electronic control unit (ECU) architecture. "Intel's AI-enhanced SDV SoCs combine the best AI PC and Intel data center technologies necessary to support a true software-defined vehicle architecture," Weast said. This consolidation promises improved efficiency, manageability, and scalability, paving the way for a more integrated and adaptable automotive ecosystem.

Intel's Open Automotive Chiplet Platform

Intel's commitment to openness extends to its chiplet platform. The company intends to work with R&D hub Imec to ensure that advanced chiplet packaging technologies meet the stringent quality and reliability requirements for automotive use. This move signifies Intel's intent to be the first automotive supplier to support the integration of third-party chiplets into its products.

The ability to integrate custom chiplets into Intel's roadmap products provides Original Equipment Manufacturers (OEMs) with flexibility and choice, reducing costs and eliminating the risk of vendor lock-in. In this way, a more scalable, software-defined architecture is made future-proof, with better innovation and collaboration within the automotive industry.

Intel's announcements at CES 2024 show a compelling picture of the future of the automobile industry. The combination of AI, sustainability, and open standards positions Intel as a driving force in shaping the next generation of vehicles. From intelligent energy management to various immersive in-car experiences, Intel's 'AI Everywhere' strategy is a testament to the company's commitment to pushing the boundaries of what is possible.

As we look ahead, the partnership with Zeekr, the collaboration with SAE International, and the commitment to open platforms and chiplet integration all point toward a future where vehicles are not just meant for transportation but intelligent, adaptable bodies.

COOLING MOSFETS FOR OPTIMAL PERFORMANCE IN DYNAMIC SYSTEMS

DEBJIT PUROHIT, SWETA KUMARI
2nd YEAR, ECE

MOSFETs deliver their maximum performance in a static regime, and their power efficiency is quite high in this configuration. However, if they are pushed in a dynamic manner, their efficiency may be reduced, and the amount of power that is lost will certainly go up. The software implementation of SPICE known as LTspice, as well as any software implementation of SPICE in general, lacks the functionality necessary to manage the thermal behaviors of an electrical circuit or a particular component. On the other hand, it is feasible to forecast a number of temperature simulations with the help of certain thermal model implementations. In this lesson, we will learn how to visualize the behaviors of a SiC MOSFET after setting its ambient temperature to a specific value.

Thermal SPICE simulations

There are new SPICE models, particularly for MOSFETs and power diodes, that can approximate the thermal behavior of an electronic component. They are easily identifiable in a simulated circuit diagram because they have two additional terminals for managing temperature-related parameters. The model includes the Tj and Tc terminals to analyze the heating of the device as a function of time. Terminal Tc represents the case temperature, while Terminal Tj represents the junction temperature.

The temperature connections function identically to the voltage terminals, with the exception that this number specifies the temperature and they are electrically isolated from the circuit. A voltage of 1 V between these terminals corresponds to a temperature of 1 C. The two terminals Tj and Tc can be used to both read and set working temperatures. In the following examples, we will specifically examine the second factor. Therefore, the voltage at node Tj contains information about the junction temperature as a function of time, which directly affects the electrical model as a function of temperature. To observe its effect on the junction, the terminal Tc must be connected to a voltage source (which indicates the case temperature) or an external RC network (heatsink model).

Analysis of the performance of SiC MOSFETs at varying switching frequencies

The practical example shown below (see circuit diagram in Figure 1) uses a SiC MOSFET model C2M0025120D with the following characteristics:

- Vds(max): 1,200 V
- Id: 63 A
- Id(pulsed): 250 A
- RDS(on): 60 mΩ
- Package: TO-247-3
- Vgs: between –10 V and 25 V
- Pd: 378 W
- Tj: between –55˚C and 150°C

The scheme shows a SiC MOSFET driving a 20-Ω resistive load with a 200-V supply. When the MOSFET is closed, a current of about 9.98 A flows through the load. In the scheme, the MOSFET is driven by a voltage of 25 V. Depending on the operation, this voltage can be fixed for static operation or pulse-width–modulated (PWM) for dynamic operation. Depending on the case, the efficiency of the MOSFET is different.

The SPICE model of the MOSFET used in the wiring diagram is peculiar in that, as mentioned earlier, it has two additional terminals that are used to manage temperature. Connecting a voltage of 25 V to its Tc terminal effectively sets the temperature of its case at 25˚C. Therefore, this value does not refer to an electrical voltage but to a temperature. With this in mind, it is now possible to verify the dissipation of the MOSFET at a given temperature and under the different conditions of static and dynamic regime.

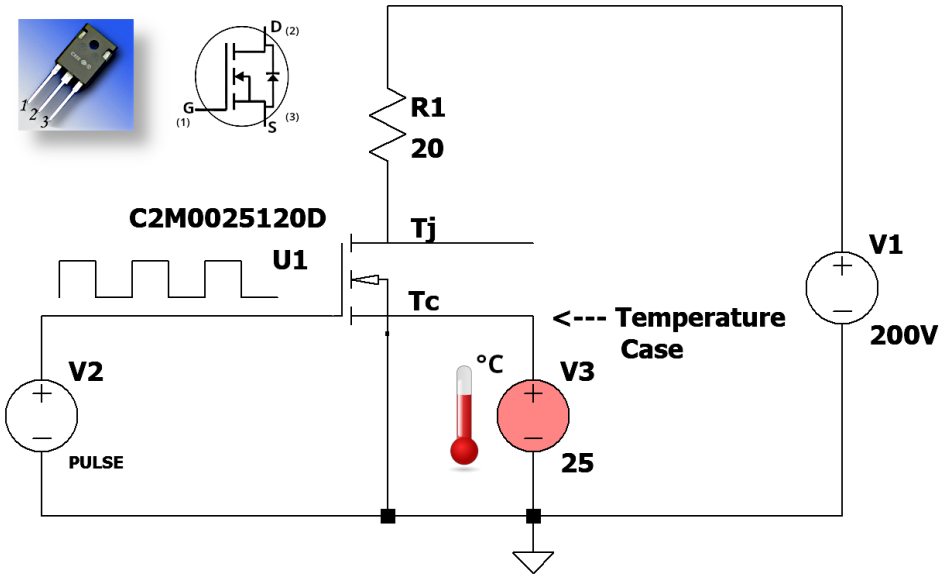

Static regime

The static regime involves driving the gate terminal with a fixed voltage (the maximum recommended by the component datasheet). In the conduction condition, the MOSFET works at its maximum efficiency, provided that the gate is driven with the correct voltage. There are, likewise, no power losses (except for the first few microseconds of conduction), as the voltage across the gate is fixed and continuous. In the diagram above, the fixed gate voltage is 25 V, and it causes the net conduction of the device. Running the simulation returns the following operating conditions:

- Current on resistive load R1: 9.98 A
- Voltage Vds: 284 mV
- Power dissipated by the MOSFET: 2.8369 W
- Power dissipated by the load: 1994.3 W
- Efficiency of the circuit: 99.857953%

As can be seen from the results in static regime, the efficiency of the system is very high due in part to the low value of the RDS (on) parameter of the MOSFET. Please note that to calculate dissipated power, the following relation can be used:

$$Pd = (Vds * Id) + (Vgs * Ig)$$
$$Pd = (0.284.09386 * 9.985795) + (25 * 2.4989988\,E-5)$$
$$Pd = 2.8375277964187\,W$$

Gate current is quite small and, therefore, negligible.

POWER-THRU ISOLATED GATE DRIVER: COMPACT & EFFICIENT GaN FET CONTROL

DEBANJAN PAL, BITTU KUMAR
1st YEAR, ECE

Allegro MicroSystems has introduced its newest device, the AHV85110 Power-Thru isolated gate driver. As the first member of Allegro's Power-Thru product family, the AHV85110 promises to deliver twice the power density with a more straightforward and effective system architecture. In comparison to Allegro's competitors' products, this driver, according to the press release, provides a single-package solution that drives GaN FETs with a footprint that is up to 50% smaller and a 40% efficiency boost. The AHV85110 eliminates EMI channels, speeds up time to market, simplifies system design, and maximizes return on investment by combining the isolated gate driver and power supply into a single package.

The standard Schottky-gate Enhancement-mode (E-mode) GaN FETs from a variety of producers, including GaN Systems, Innoscience, ST, Nexperia, GaN Power International, Taiwan Semiconductor, Rohm, and others, are specifically tailored for use with the AHV85110 driver. Additionally, it can power some Transphorm cascode-GaN devices that contain low-voltage logic-level MOS components. At 6 V VGS (Gate-to-Source Voltage), the driver can drive up to 30 nC. With this functionality, switching activities involving GaN FETs are controlled effectively and consistently.

Standard Schottky-gate Enhancement-mode (E-mode) GaN FETs are designed specifically for the AHV85110 driver and are available from a number of manufacturers, including GaN Systems, Innoscience, ST, Nexperia, GaN Power International, Taiwan Semiconductor, Rohm, and others. Additionally, some Transphorm cascode-GaN devices with low-voltage logic-level MOS components can be powered by it. The driver can drive up to 30 nC at 6 V VGS (Gate-to-Source Voltage). GaN FET switching operations are effectively and consistently regulated by this feature.

In an interview with Power Electronics News, Vijay Mangtani, Vice President – Power ICs at Allegro Microsystems, said that in the market, there are concerns regarding gallium nitride (GaN) compared to silicon carbide (SiC). Wide-bandgap silicon-carbide (SiC) and gallium-nitride (GaN) field-effect transistors (FETs) may be more efficient at the system level, but they are often hard to integrate. Conventional gate driver implementations necessitate an isolated gate driver and an isolated power supply. When assembled, the connections between the driver, power source, and FET can create electromagnetic interference (EMI) pathways that degrade performance. Mitigating these effects can add design complexity, time, and cost to a project's schedule and increase the solution's size and weight.

"Allegro MicroSystems is focusing on enabling GaN technology with its first-generation devices while aiming to address concerns in future generations. Allegro MicroSystems' core expertise lies in BCD technology, innovative packaging, isolation capabilities, and a strong automotive background. Their focus on electric vehicle applications includes onboard chargers, DC-DC converters, thermal management, inverters, and battery management. The company brings innovation to high-frequency current sensing with magnetic sensors that offer power loss reduction, speed, and accuracy. With a customer-centric approach, Allegro collaborates closely with clients to address specific challenges and provide tailored solutions for their EV systems," said Mangtani.

He added, "Our team is skilled in developing innovative packaging solutions that enhance the performance and reliability of our products. We design packages with advanced thermal management and isolation capabilities, ensuring optimal operation in challenging environments. Moreover, we excel in providing isolation solutions within our packages, which is crucial for applications requiring high-voltage protection and noise reduction. Our isolation technologies guarantee safe and reliable operation, especially in automotive and industrial systems."

The single magnetic isolation barrier in the AHV85110 driver efficiently transfers both the PWM signal and the gate power. This reduces the total parasitic capacitance between the primary and isolated sides by a large amount. This combined capacitance for signal and power channels is typically less than 1 pF. In contrast, traditional isolated gate drivers with separate isolated DC-DC bias supplies can have up to 10 pF or more parasitic capacitance because the DC-DC isolation transformer adds to it.

Technology

The global renewable energy movement requires automotive and industrial power system designers to generate, store, and use energy more efficiently. The trade-off between reducing weight and size while keeping costs in check is a critical consideration for every system in the electric vehicle space. As demonstrated with their current sensors, Allegro's approach of integrating complex circuits into a single package can help streamline designs and optimize system performance. Safety, efficiency, and size become paramount in specific applications such as direction inverters and onboard chargers. Allegro's ability to eliminate multiple components, including transformers, and reduce the number of PCBs can lead to more compact and efficient designs. Time-to-market is another crucial aspect, considering the competitive nature of the market. Allegro's philosophy of providing easy-to-use solutions that address layout challenges, EMI concerns, and other complexities can be instrumental in helping customers accelerate their product development and gain a competitive edge.

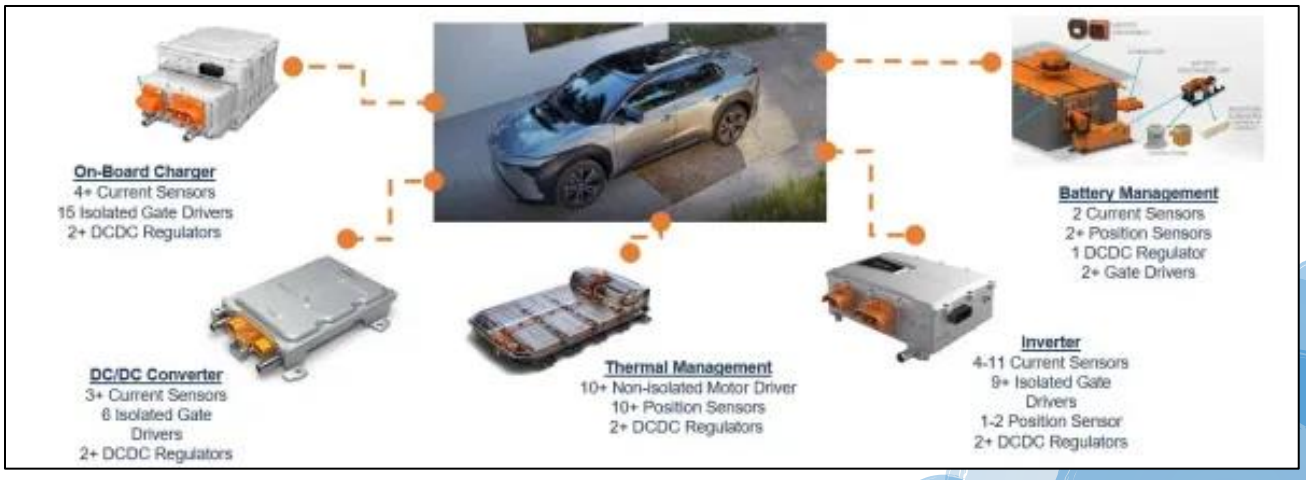

LOW-POWER HIGH-FREQUENCY WPTS LOSS ANALYSIS

ADITYA KUMAR, SUBHAM KUNDU
2nd YEAR, ECE

Wireless power transfer systems (WPTS) for wearable and portable applications are becoming increasingly popular as the demand for wireless mobile phone and smartwatch adapters rises. Due to the extremely low coupling factor (0.1) between the primary transmitting (Tx) coil and the secondary receiving (Rx) coil in such applications, it has been extremely difficult to achieve high efficiency. In addition, the proliferation of battery-powered consumer electronics has significantly increased interest in the development of charging platforms for multiple receivers. Recently, there has been a drive for such applications to operate in the restricted and unlicensed lower ISM band at 6.78 MHz.

Numerous scholarly works on this topic have only addressed the optimization of transmitter and/or receiver modules. In addition, WPTS efficiencies are provided as experimental data without any preliminary investigation into the impact of silicon devices on the primary and secondary portions of the system. Therefore, the primary objective of this research is to develop an efficient model for the analysis and efficiency evaluation of WPTSs, including all semiconductor device losses pertinent to low-power wearable device applications. This article presents an analytical model based on the first harmonic solution of a WPTS, along with its solution, simulation results, and experimental measurements for a 2-W @ 6.78 MHz WPTS.

WPTS modeling and numerical solutions

The WPTS mentioned henceforth refers to the architecture in Figure. It can work with a primary constant frequency and a secondary PWM control ensuring duty-cycle and phase-shift modulation. The authors aim to calculate the output current (I_{out}) and WPTS efficiency given the output voltage (V_{out}) and the fire angles of the MOSFETs Q_1, Q_2, Q_3 and Q_4.

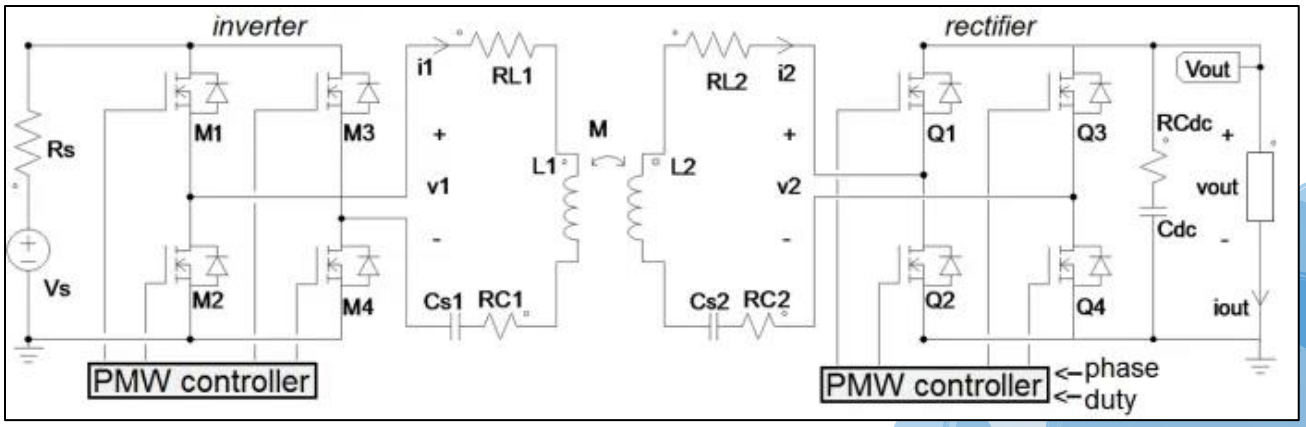

The relations among phase-lag (ϕ), the angle between zero-crossing current (i^2t) and falling voltage (v^2t) denoted by α, the angle between the rising voltage (v^2t) and (i^2t) denoted by β and Dare given by Equation 1, where D = 1 – ($\alpha \div \beta$) $\div \pi$ and $\phi = (\alpha - \beta) \div 2$.

$$\alpha = \tfrac{1}{2}\left[\pi(1-D)\right] + \phi \quad ; \qquad \beta = \tfrac{1}{2}\left[\pi(1-D)\right] - \phi$$

For unidirectional operations, values of practical interest for α and β are the ones ensuring 0 < D < 1 and $-\pi \div 2 < \phi < \pi \div 2$. Given V_s, α, β and the capacitances C_{S1} and C_{S2}, the WPTS output power and efficiency are influenced by the system's total losses. Considering the WPTS first harmonic solution:

$$v_1(t) = V_1 \cos(\omega_s t + \phi_{V_1}) \qquad i_1(t) = I_1 \cos(\omega_s t + \phi_{I_1})$$

$$v_2(t) = V_2 \cos(\omega_s t + \phi_{V_2}) \qquad i_2(t) = I_2 \cos(\omega_s t + \phi_{I_2})$$

The instant where i2t crosses zero with the positive derivative is the reference for the phase angles. The equations for the WPTS Tx-Rx coupled loops are:

$$\bar{V}_1 = \dot{Z}_1 \bar{I}_1 - j\omega M \bar{I}_2 \qquad \bar{V}_2 + \dot{Z}_2 \bar{I}_2 = j\omega M \bar{I}_1$$

Where:

$$\bar{V}_1 = V_1 e^{j\phi_{V_1}}, \quad \bar{I}_1 = I_1 e^{j\phi_{I_1}}, \quad \bar{V}_2 = V_2 e^{j\phi_{V_2}}, \quad \bar{I}_2 = I_2 e^{j\phi_{I_2}}$$

$$\dot{Z}_1 = R_{L_1} + R_{s_1} + 2R_{dson}^{inv} + j\omega L_1 + \left(j\omega C_{s1}\right)^{-1} = Z_1 e^{j\phi_{Z_1}}$$

$$\dot{Z}_2 = R_{L_2} + R_{s_2} + 2R_{dson}^{rec} + j\omega L_2 + \left(j\omega C_{s2}\right)^{-1} = Z_2 e^{j\phi_{Z_2}}$$

Applying Fourier formulas to the Tx and Rx voltages and currents provides:

$$V_1 = \frac{4}{\pi} V_{in} \quad ; \quad V_2 = \frac{V_{out}}{\pi}\sqrt{8\left[\cos(\alpha)\cos(\beta) - \sin(\alpha)\sin(\beta)\right]}$$

$$\phi_{V_2} = \phi_{I_2} - \frac{1}{2}(\alpha - \beta) = -\frac{1}{2}(\pi - \alpha + \beta)$$

Merging Equations 3 and 5, we get Equations 6 and 7:

$$\Gamma_{re} = \omega M V_1 \cos\left(\phi_{V_1} + \tfrac{\pi}{2}\right) - Z_1 Z_2 I_2 \cos\left(\phi_{Z_1} + \phi_{Z_2} + \phi_{I_2}\right) + -\omega^2 M^2 I_2 \cos\left(\phi_{I_2}\right) - V_2 Z_1 \cos\left(\phi_{V_2} + j\phi_{Z_1}\right) = 0$$

$$\Gamma_{im} = \omega M V_1 \sin\left(\phi_{V_1} + \tfrac{\pi}{2}\right) - Z_1 Z_2 I_2 \sin\left(\phi_{Z_1} + \phi_{Z_2} + \phi_{I_2}\right) + -\omega^2 M^2 I_2 \sin\left(\phi_{I_2}\right) - V_2 Z_1 \sin\left(\phi_{V_2} + j\phi_{Z_1}\right) = 0$$

Z_1, Z_2, V_1, M, ω, ϕ_{Z1}, ϕ_{Z2} and ϕ_{I2} are all known. From Equation 5, V2 and ϕV2 are functions of and V_{out}. Given Vs, V_{out} and the only two functions I_2 and ϕ_{V1} are determined by solving the nonlinear equation system of Equations 6 and 7 by using the Newton-Raphson algorithm to avoid simplified approximations.

Neglecting rectifier switching losses, the authors calculated the average output current (I_{out})of the rectifier as:

$$I_{out} = I_{rect,av} = \frac{1}{T_s}\int_{\alpha}^{\pi-\beta} I_2 \sin(\vartheta)d\vartheta = \frac{1}{\pi} I_2\left[\cos(\alpha)+\cos(\beta)\right]$$

Considering that a part of I_{out} is lost because of the MOSFET switching losses:

$$I_{out,net} = I_{out} - I_{sw,rec}$$

The switching current ($I_{sw,rec}$) can be considered as sought by an equivalent dissipative current source connected in parallel to the rectifier output. Such current effectively allows analysis of the impact of rectifier switching losses on the output power and efficiency of the WPTS. Accordingly, the equivalent current $I_{sw,rec}$ is given by:

$$I_{sw,rec} = \left(P_{on-off,rec} + P_{gate,rec} + P_{body,rec}\right)\Big/ V_{out}$$

From Equations 8, 9 and 10, the net output current ($I_{out,net}$), accounting for the effect of the rectifier MOSFET losses, is determined. $I_{out,net}$ results correlate to the current I_2 through a nonlinear equation, which is also dependent on the sign of fire angles and . Given and, the rectifier I_{out} versus V_{out} curve, which also represents the output characteristic of the WPTS, can be determined for different rectifier MOSFETs to identify the device, ensuring the best power and efficiency performance.

The Tx current I_1 can be determined by:

$$\bar{I}_1 = \left(\bar{V}_1 + j\omega M \bar{I}_2\right)\Big/ \dot{Z}_1$$

The inverter switching losses $P_{sw,inv}$ were modeled by means of an equivalent current source in parallel to the inverter input, whose current is given by:

$$I_{sw,inv} = \left(P_{on-off,\text{inv}} + P_{gate,inv} + P_{body,inv}\right)\Big/ V_s$$

The Tx and Rx conduction losses are given by:

$$P_{Tx} = \left(R_{s_1} + R_{L_1}\right) I_{1,rms}^2 \qquad P_{Rx} = \left(R_{s_2} + R_{L_2}\right) I_{2,rms}^2$$

The overall WPTS efficiency is evaluated as:

$$\eta = \frac{V_{out} I_{out,net}}{V_{out} I_{out,net} + P_{con,inv} + P_{sw,inv} + P_{Tx} + P_{Rx} + P_{con,rec} + P_{sw,rec}}$$

OPTIMIZING CONTROL OF POWER CONVERTERS

AQDAS SULTAN, POOJA YADAV
1st YEAR, ECE

Controlling power converters is an essential component in maximizing the overall performance of power-conversion systems. Effective management of power converters can lead to enhanced component life, decreased energy losses, and optimized efficiency. Sophisticated control algorithms enable the efficient and optimal management of power transitions, while simultaneously maintaining a constant output voltage and current of the power converter.

The capability of power converter control to adjust to dynamic fluctuations in load conditions and power-source attributes is a critical component. This feature enables the power converter to deliver a consistent and constant output, irrespective of fluctuations in power requirements or environmental factors. Furthermore, power converter control may encompass several sophisticated functionalities, including the ability to modify the output waveform, compensate for harmonic distortion, and manage power quality. These characteristics enable customization to suit the particular requirements of the application and guarantee a dependable, superior power supply.

Ongoing advancements in power converter control research and development yield novel methodologies and more intricate algorithms. The integration of sophisticated digital controllers with machine learning-driven intelligent control algorithms is creating novel opportunities to enhance the functionality of power electronic converters. The method of pulse-width modulation (PWM) is extensively employed in the regulation of power converters. This method of control entails the generation of a signal that activates and deactivates the electronic switches of the power converter in order to produce the desired output voltage.

The switching function, illustrated in Figure, is accomplished through the comparison of two signals: the carrier and the modulant. A concise summary of these two signals is as follows:

- The modulant, which contains the precise information regarding the desired output voltage, is a signal.
- The carrier, which typically takes the form of a triangular wave, is a periodic signal whose switching frequency is equivalent to that of the power converter.

Through the interaction between these two signals, the switching function is generated. As a demonstration, the system depicted in the figure consists of three types of generators, some real and some calculated and processed:

- v(1) is a triangular signal, referred to as "carrier." It is a periodic and usually fixed-frequency signal. Depending on the needs, its form may be different.
- v(2) is a threshold voltage, referred to as "modulating" (or reference voltage). It decides the switching threshold level of the output logic states. It can be chosen by the user or can be of any waveform, such as sinusoidal in the case of operation as an inverter.
- v(3) is the switching voltage that is the result of the intersection and comparison of the first two signals. It is called the binary switching function. Usually, if the modulant is greater than the carrier, it will have a value of 1. In the opposite case, it will have a value of 0. The comparison can be performed via hardware, with fast comparison circuits, or via firmware, through the use of powerful microcontrollers.

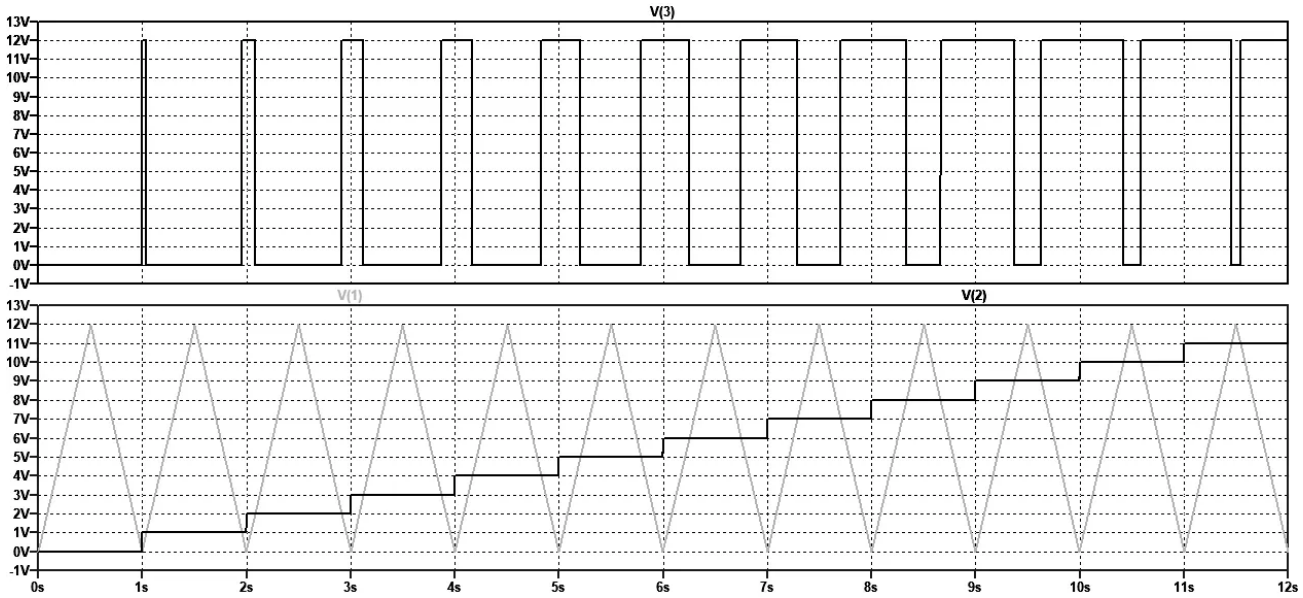

The result of the switching function is sent directly to the driver, which manages the switching on and off of the power converter switches according to the sequence of 1 and 0 of the switching functions. As can be seen, therefore, the result is a true PWM signal arising from the presence of two distinct and easily controlled signals. The basic principle of PWM is to vary the pulse width of the switching signal proportionately to the desired reference voltage. This allows the effective output value of the power converter to be controlled, ensuring proper regulation and high quality of the power signal. The use of PWM, achieved as described above, offers numerous advantages, including high energy efficiency, improved output signal quality, the ability to control output power and reduced power losses.

In the example just seen, with respect to the triangular-shaped carrier, the duty cycle of the output signal linearly follows the level of the modulant, according to the following linear relationship:

$$\%duty = \frac{V_{max}}{V_{mod}} = \frac{V_{max}}{V_{(2)}}$$

DESIGN CHALLENGES OF BATTERY POWERED IoT DEVICES

SOMNIL NEOGI, PRINCE KUMAR
3rd YEAR, ECE

Applications for the Internet of Things (IoT) are created on smart, networked, and most likely battery-powered electronic devices that send pre-processed data to a cloud-based infrastructure. An IoT device collects data, processes it, and then transmits it back to a hub or another network node using a variety of embedded components, such as processors, communication ICs, and sensors. This can include anything from a simple temperature sensor that transmits the current room temperature to a central monitoring point to a machine health monitor that monitors the long-term performance information of very expensive production machines.

IoT Applications

IoT devices have virtually endless use cases. Smart transmitter applications gather data about their environment before making decisions such as controlling the temperature, issuing alerts, or automating procedures. A control center receives precise measurements from portable equipment like air quality measurement systems and gas meters via the cloud. Another application is GPS tracking technology. They make it possible to track both animals and cargo containers by using smart ear tags. They represent a very small percentage of devices connected to the cloud. Additional uses include wearable health care and infrastructure sensors. Applications for the Industrial Internet of Things are a crucial area of growth in the Fourth Industrial Revolution.

Design Challenges

Running power to most IoT nodes is not an option because they are typically placed out of sight or in challenging locations. This indicates that batteries and/or energy gathering are their sole power source.

Large facilities can be highly expensive to move power around. Take the case of a remote IoT node in a factory as an illustration. The only remaining alternatives for powering these remote nodes are battery power or energy harvesting, because installing a new power cable would be expensive and time-consuming.

The device's total cost of ownership is impacted by the necessity to adhere to a strict power budget to maximize the battery's lifespan. The requirement to replace the battery once its life has passed is another drawback of battery use. Included in this is the price of the battery itself, as well as the likely high expense of hiring workers to replace and possibly get rid of the old battery.

Also, overdesigning the battery increases its size and expense. Thus, it is crucial to optimize the power budget and reduce energy consumption wherever feasible to install the smallest battery while still meeting your design requirements. There are three main types of power sources for IoT applications:

- Devices that rely on non-rechargeable battery power (primary battery)
- Devices that require rechargeable batteries
- Devices that utilize energy harvesting to provide system power

Primary Battery

In these applications, the device periodically wakes up before returning to a power-efficient deep-sleep state. Its power source's high energy density and straightforward construction are key benefits. Batteries are not ideal for situations where power consumption is slightly higher, though, as they have a limited lifespan.

Making the best use of the energy offered by different power sources is the main difficulty from a design standpoint. Making a power budget plan is crucial to maximizing the battery's lifespan, with 10 years being a typical lifetime goal.

A low-power DC-to-DC converter, such as the Analog Devices LTC3336, with an extremely low quiescent current (a few nanoamperes) is a typical device ideal for non-rechargeable battery-powered IoT devices.

The LTC3337, a nano-power primary battery state-of-health monitor and coulomb counter, is the companion device of the LTC3336. Just strap the IPK pins in accordance with the peak current necessary in the 5-mA to 100-mA range to utilize this device in a new design. Perform a few computations using your chosen battery, then fill in the recommended output cap using the chosen peak current from the datasheet.

Rechargeable Battery

Rechargeable batteries are a good solution for higher-power or higher-drain IoT applications in which frequent replacement of the primary battery is not an option. Due to the initial cost of the batteries and the charging electronics, rechargeable battery applications are more expensive. Still, in higher-drain applications in which the batteries are regularly discharged and recharged, the expense is justifiable and quickly recouped. Another option, but mainly for short-term backup storage, is a capacitor or supercapacitor, depending on the power requirements.

BEFORE SWITCHING YOUR SOLAR PANEL, TRY CHANGING ITS TILT

SUPRIYA YADAV, ANUSUYA CHATTERJEE
1st YEAR, ECE

We occasionally have to decide whether to purchase larger solar panels in order to generate more energy. This isn't always the greatest option, though. In many circumstances, altering and improving the tilt of the solar panels may be preferable than increasing their size. In this post, we'll examine the significance of solar panel tilt and how it may impact energy output.

The strength of the incident light

The quantity of solar energy that solar panels can gather depends greatly on their tilt with respect to the sun. The photovoltaic system's geographic location affects the proper tilt. You should position the panels in the direction where the incidence of the rays is most concentrated, avoiding shade as much as possible, to get the highest output from your solar system and maximize its energy. During the time of solar irradiation, this state should be maintained. Installing a solar tracker system, which enables the solar panels to be orientated appropriately depending on the season and time of day, is the ideal choice. However, this technique is not particularly practical because of the cost. However, this article only looks at the mathematical and physical elements of the problem, not the economic one.

Mathematics helps us choose the direction and angle

Mathematics can help choose the optimal direction and angle for solar panel installation to maximize the amount of energy produced. Specifically, trigonometry is a branch of mathematics that can be used to calculate the ideal tilt angle of solar panels, based on latitude and time of day. There are some simple formulas and tables that can help to best place solar modules. The following formula is extremely simple and is used to calculate, roughly, the solar panel tilt in both summer and winter.

$$\theta_{winter} = \text{latitude} + 15$$
$$\theta_{summer} = \text{latitude} - 15$$

Of course, these are fairly generic positions that assume a static position of the modules. Another method, which is slightly more accurate than the one just mentioned, allows the generic solar panel tilt to be calculated in one of four seasons (winter, summer, spring and autumn).

$$\theta_{winter} = \text{latitude} \cdot 0.9 + 29$$
$$\theta_{summer} = \text{latitude} \cdot 0.9 - 23.5$$
$$\theta_{spring} = \text{latitude} - 2.5$$
$$\theta_{autumn} = \text{latitude} - 2.5$$

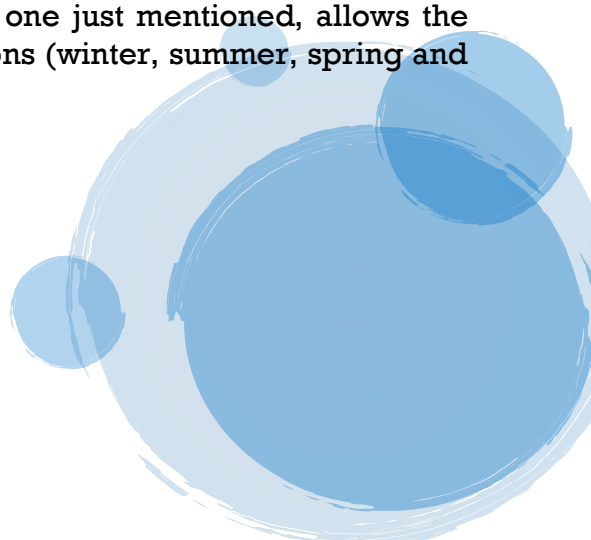

With these formulas, the results are even better adapted to different seasonal conditions.

Figure helps us to understand this phenomenon. Depending on its inclination with respect to the plane, it is distributed differently, and because its energy is constant, the concentration per unit area is different. The closer you get to the poles, the more the same light is distributed over a greater area and its relative power is lower. At the equator, in fact, there is a higher temperature than at the poles.

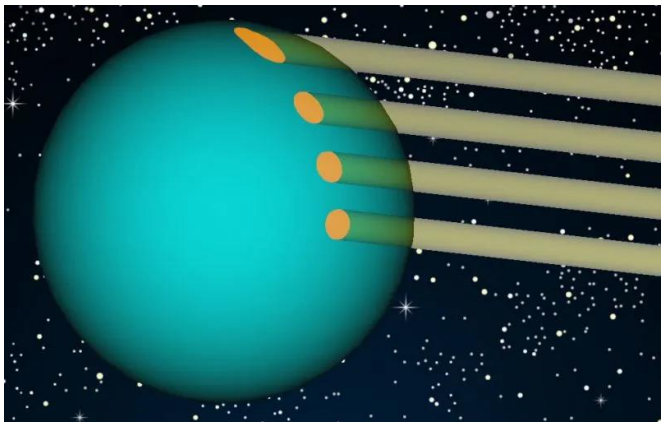

The angle that makes a difference

Under ideal conditions, with the sun placed perpendicular to the solar panel, the amount of solar power dependent on it is about 1,000 W/m². This does not mean that such a panel can produce an actual power of 1,000 W. The value is much less, as most of the energy is infrared rays that generate heat. A plane oriented directly toward a source receives the maximum amount of light. But if the angle of the plane changes, the amount of light hitting a unit area decreases in proportion to the cosine of that angle. A general formula for calculating the energy of the light on the plane (both visible and infrared) is as follows:

$E = I \cdot \cos(\theta)$

Where E is the amount of light energy in W/m^2, I is the solar radiation in W/m2, θ is the angle of incidence of light on the plane (that is, the angle between the direction of the light and the normal to the plane) and cos(θ) represents the cosine function.
With such a relationship, the following table can be created:

Angle	Cosine of angle
0	1.000000
10	0.984807
20	0.939692
30	0.866025
40	0.766044
50	0.642787
60	0.500000
70	0.342020
80	0.173648
90	0

Therefore, a solar panel must be oriented to capture maximum light, which is achieved when its plane is perpendicular to the direction of light.

TINY ORGAMI BASED FLYING ROBOTS ENABLE NEW SENSOR APPLICATIONS

MUSKAN KUMARI, NIKITA YADAV
2nd YEAR, ECE

Small robotic devices have been developed by researchers at the University of Washington that can modify the way they fly through the air by folding themselves into a more compact form while they are descending. Each unit has a controller, an onboard battery-free actuator, and a solar power-harvesting circuit to bring about these form changes while they are in flight. During the descent, the apparatus is capable of switching between an unfolded and a folded configuration, which enables us to control its trajectory.

When the microfliers (shown in Figure) are released from a drone, they employ a special origami fold called the Miura-ori to change their flight pattern from one in which they tumble and disperse themselves outward through the air to one in which they fall directly to the ground. The researchers can regulate the timing of each device's transition by selecting one of three possible techniques. These methods are an onboard pressure sensor (which estimates altitude), an onboard timer, or a Bluetooth signal. This allows the researchers to spread out the fliers.

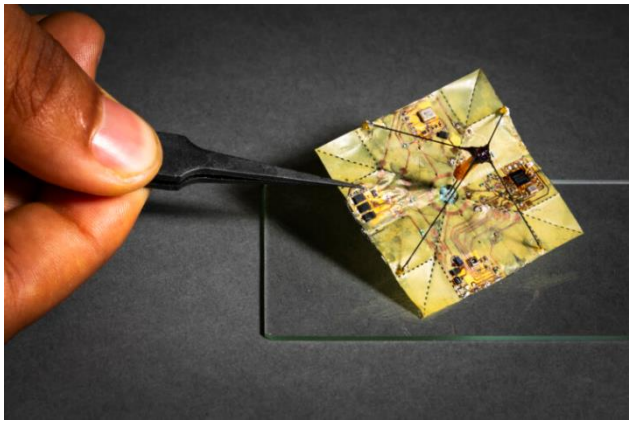

Microfliers' main features

The ability of the battery-free microfliers to change shape while in flight to adjust the distance over which they disperse their payload is the most notable characteristic of these tiny flying devices. With the use of a bi-stable leaf-out structure, the microflier can follow one of two entirely distinct falling behaviors:

- As shown in Figure, the microflier demonstrates a tumbling behavior when unfolded and flattened, which causes an increase in lateral displacement in the wind.
- The microflier's orientation is stabilized when it is folded inward, which leads to a descent that is comparatively less susceptible to wind influence.

Electronic circuits are constructed and patterned directly into the flexible material that makes up the device, as shown in Figure 2. This allows the transition between the two stable states to be controlled. To be more specific, the command to fold or unfold is carried out by a low-power electromagnetic actuator that generates peak forces of up to 200 millinewtons in a span of under 25 milliseconds while being fueled by solar cells.

The circuits embedded directly into the folded origami structure include the following components:

- Programmable microcontroller
- Bluetooth radio transceiver
- Solar power harvesting circuit
- Pressure sensor (used for estimating the altitude value)
- Temperature sensor.

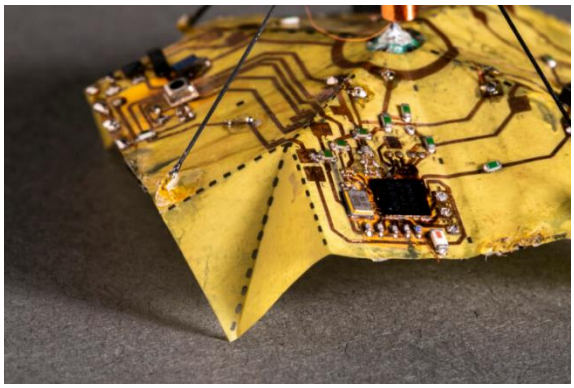

The 414-milligram origami microfliers that were developed by UW researchers have been demonstrated to be able to electronically change their shape while they are in flight, travel up to 98 meters in a light breeze, and wirelessly transmit data via Bluetooth up to 60 meters away using only the power that is collected from the sun during experimental tests that were carried out outdoors.

By integrating power harvesting and minuscule actuators with a fold inspired by the geometric patterns observed in leaves, these tiny robotic devices simulate the flight of various leaf types in midair. Comparable to an elm leaf, the unfolded, flat origami structure tumbles erratically in the breeze. Alternately, assuming the folded position alters the surrounding atmosphere and facilitates a steady fall, analogous to how a maple leaf descends. This previously unattainable feature allows for battery-free regulation of microflier descent via this remarkably energy-efficient method.

Different design challenges have been overcome during the design of these robotic systems, such as:

- Avoid accidentally transitioning to the folded state before this operation is commanded.
- Perform the transition between the unfolded and folded state in a short time. According to the researchers, the onboard actuators currently need only about 25 milliseconds to initiate the folding.
- Alter its shape while detachable from an external power source. The power-harvesting circuit of the microfliers supplies the actuator with energy via sunlight.

Another relevant characteristic of the microfliers, which paves the way to a wide range of interesting applications, is their capacity to carry onboard sensors to survey temperature, humidity, and other conditions while soaring. Combined with their ability to switch among two stable descent configurations, microfliers may, in the future, help change the way scientists study agriculture, meteorology, climate change, and more.

Origami in the aerospace industry

The use of origami in the aerospace industry is nothing new. The 'Miura-ori' technique, used by the microfliers developed by UW's researchers, has already been explored to fold and open solar panels used in space missions. The main feature of this folding system is that it has only one degree of freedom, allowing a folded structure to be opened with a single pull motion.

Initially devised by Japanese astrophysicist Koryo Miura, this technique has been analyzed and perfected by researchers from aerospace agencies, including NASA's Jet Propulsion Laboratory (JPL), for application to space solar panels. The advantage of this technique is that there is only one way to open and close the structure and the operation requires minimal effort.

Applications

The microfliers are mechanically bi-stable, but at the time, the actuator is the only thing that can make them transition from their chaotic (dispersing) state to their stable (falling straight down) state. Hysteresis is robust enough to forestall unintended changeover during free fall.

The present generation of microfliers only allows for one transition, from the tumbling to the falling state, but future devices will allow for transitions in either direction. The researchers claim that the new features would improve landing precision even in strong winds.

Microfliers that are distributed in the wind like seeds and leaves are useful for automating widespread sensor deployments. Microfliers can be used to gather data on the atmosphere's temperature, illumination, and other characteristics as they descend. Research into fields like digital agriculture and climate change monitoring could benefit from a network of these microfliers.

Microfliers approach is innovative. Drone-controlling devices such as motors are cumbersome and weighty, and even insect-inspired wings that are minuscule prove to be arduous to power using the meager energy that small solar cells can generate. The researchers adopted an unconventional approach in this endeavor, relying on the distinctive characteristics of origami structures to fabricate battery-free origami microfliers capable of undergoing shape changes while in flight.

This methodology creates a novel realm for design, allowing for precise landing locations and control over the descent's trajectory, among other capabilities. The researchers aspire for this study to serve as an initial stride towards a future realization of a novel category of pilots and flight modalities.

FINLAND SCALES UP QUANTUM COMPUTING WITH A 20-QUBIT SUPERCONDUCTIVE DEVICE

TAMAZIT HAZRA, SOUVIK MAITY
1st YEAR, ECE

The state-owned VTT Technical Research Centre of Finland, a pioneering innovation and research collaborator for businesses and society, has unveiled the second quantum computer in Finland: a 20-qubit superconductive apparatus. The quantum computer is the outcome of a rigorous collaborative effort between VTT and IQM Quantum Computers in technology development, showcasing the companies' exceptional proficiency in devising scalable quantum computer technologies.

Finland declared its intention to develop a 50-qubit quantum computer by 2024 and allocated a total of 20.7 million euros from the government towards this end, as disclosed in November 2020. The development will continue in the coming years, as the Finnish government has allocated a total of 70 million euros in funding to increase the quantum computer's qubit count to 300 and achieve quantum advantage. The addition of the 20-qubit quantum computer to Finland's arsenal of quantum computing investment assets fortifies the nation's standing. The inaugural 5-qubit quantum computer developed by Finland was finalized in 2021.

Superconductive quantum computer

A superconductive quantum computer (QC) is a type of quantum computer that performs quantum computations using superconducting circuits. By applying the tenets of quantum mechanics, quantum computers are capable of performing information processing operations that classical computers are unable to. Quantum computers that operate on superconducting materials, which can conduct electric currents with zero resistance, are capable of generating and manipulating qubits, the fundamental units of quantum data.

The field of superconducting quantum computing is characterized by high dynamicity, with researchers continually exploring new materials and fabrication techniques to improve the performance, coherence times, and scalability of superconducting qubits. Indeed, choosing the right materials is crucial, as they need to exhibit superconducting properties at extremely low temperatures, typically close to absolute zero. Moreover, this aspect requires sophisticated and expensive cooling systems to maintain the superconducting state of the qubits.

Even though this sector is rapidly evolving with new advancements and discoveries, here are some of the most commonly used materials in superconducting quantum computers:

- **Niobium (Nb):** Niobium is an extensively utilized superconducting material, and alloys composed of niobium are commonly used to construct resonators and qubits that conduct electricity. Thin films of niobium, a material that is frequently employed due to its comparatively elevated critical temperature (the temperature at which a substance transitions to superconductivity), are well-known.
- **Yttrium Barium Copper Oxide (YBCO):** YBCO, a superconductor operating at elevated temperatures, has been investigated for potential use cases in quantum computing. Although the majority of superconducting quantum computers function at exceedingly low temperatures, the implementation of high-temperature superconductors such as YBCO may offer the possibility of streamlining the cooling demands.
- **Aluminum (Al):** Another prevalent superconducting material utilized in quantum computing is aluminum. Josephson junctions constructed from aluminum are critical constituents in superconducting qubits. Utilizing the Josephson effect, which is observed in superconducting systems, superconducting circuits are manufactured.
- **Josephson Junctions:** Josephson junctions are an essential type of device in superconducting quantum computers and not a singular material. Typically, niobium or aluminum is employed to encapsulate a thin insulating barrier between two superconducting layers in the fabrication process. In superconducting circuits, Josephson junctions are employed to generate non-linear components, thereby facilitating the deployment of quantum gates.
- **Titanium Nitride (TiN):** An additional substance utilized in constructing superconducting circuits is titanium nitride. Frequently employed in resonators and other electronic components on account of its exceptional conductivity.

Designed for scalability

Starting from the initial steps, the new quantum computer has been designed to enable the scaling up of the system, passing from the now completed 20-qubit quantum computer (see Figure) to 50-qubits. The update is scheduled to be completed by the end of 2024, according to plans made by VTT and IQM.

VTT, a Finnish research and technology organization with nearly 80 years of expertise, has set the extremely ambitious objective of constructing three quantum computers within four years using solely local industry. The first objective, the development of a 5-qubit quantum computer, has been met, and the second objective, the deployment of a 20-qubit quantum computer, has been now achieved; today, work is underway on developing a 50-qubit quantum computer.

IQM Quantum Computers claims that this is a breakthrough for their company, the country of Finland, and the European quantum community as a whole. The introduction of the 20-qubit quantum computer is a major milestone, and plans are well on for creating the next generation of processors with 54 qubits and beyond for sale to customers. As IQM is a European quantum leader contributing to the strategic European agenda, they will continue to foster collaboration and engage diverse stakeholders to drive more investments in helping the ecosystem scale up and become more competitive.

The first 54-qubit quantum computer is being built by IQM and VTT in Finland, while a quantum computer is being built in Germany by a partnership lead by IQM (Q-Exa) and designed to be integrated into an HPC supercomputer to serve as an accelerator for future scientific research.

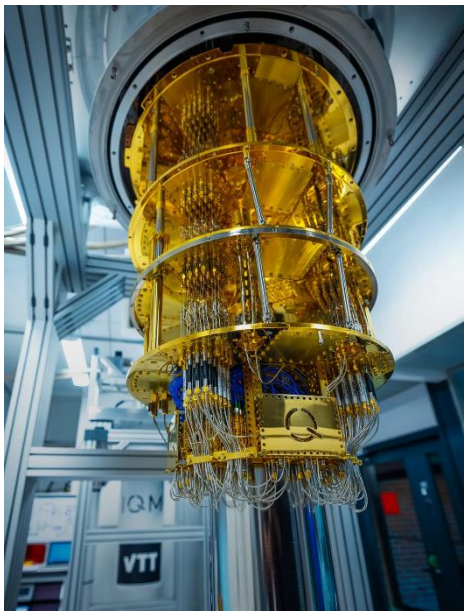

VTT's Research Manager Pekka Pursula says the team has made significant advancements in integration methods and signaling. They've also figured out how to manufacture and package qubits so that more of them can fit on a silicon chip and the electrical signals can be sent at temperatures near absolute zero. There are currently 20 qubits on a silicon chip in the new quantum computer, but they have developed the integration methods to make that number much larger.

Micronova, Finland's national research facility for micro and nanotechnology, is where VTT's new 20-qubit quantum computer may be found. A 5-qubit quantum computer, Finland's first, can be found in the same building. Located in Espoo, Finland, Micronova possesses the most expansive research and development cleanroom among the Nordic countries. The facility, which is jointly operated by VTT and Aalto University, is a component of OtaNano, the Finnish national research infrastructure for micro, nano, and quantum technology.

Micronova serves as a pivotal node within the ecosystem of the Finnish electronics industry. In addition to processing capabilities for silicon-based CMOS, MEMS, and photonics devices, the cleanrooms also support thin film components and 3D integration. Researchers create and develop state-of-the-art quantum devices and photonics components, passive RF components, PMUTs, and other MEMS devices within the cleanrooms of Micronova.

EXPLORING Wi-Fi 7 NEW CAPABILITIES AND APPLICATIONS

RANIT ROY, SHRUTI KUMARI
2nd YEAR, ECE

"Get Ready for Wi-Fi 7: Applying New Capabilities to the Key Use Cases", a report examining how this new technology will revolutionize people's daily lives throughout the world, was recently released to the public by the Wireless Broadband Alliance (WBA).

The Wireless Broadband Alliance (WBA) mission, founded in 2003, is to facilitate seamless, interoperable Wi-Fi service experiences within the global wireless ecosystem. To attain this vision, WBA's mission is to facilitate collaboration between service providers, technology companies, cities, regulators, and organizations.

Wi-Fi 7, which is based on the IEEE 802.11be (Extreme High Throughput) standard, has a plethora of cutting-edge features that will either enhance previously feasible uses or make possible uses that were previously impossible with current wired and wireless technologies.

Wi-Fi 7 key features

The report, which was led by WBA members Broadcom, CableLabs, Cisco, and Intel, investigates a number of the most significant new capabilities and applications offered by Wi-Fi 7, including the following:

- Wi-Fi 7 has double the bandwidth and triple the performance of Wi-Fi 6 (802.11ax).
- Enhanced support for applications that are sensitive to latency.
- Wi-Fi 7 supports up to 320 MHz channel frequencies, whereas Wi-Fi 5 and Wi-Fi 6 are limited to 160 MHz. It also supports 4k QAM, an improvement over previous standard. Wi-Fi 7 can deliver speeds over three times quicker than Wi-Fi 6 due to its wider channels and 4K QAM support. This is essential for enabling multi-Gigabit Wi-Fi service throughout the entire household.
- Wi-Fi 7 devices can use multi-link operation (MLO) in the 2.4 GHz, 5 GHz, and 6 GHz bands to increase throughput by aggregating multiple links or to swiftly transfer critical applications to the optimal band by switching between links without interruption.
- Using the fast link switching feature, Wi-Fi 7 devices avoid interference and access Wi-Fi channels without postponing mission-critical data transmission. Wi-Fi 7 is also ideal for immersive XR/AR/VR, online gaming, and other consumer applications that require high throughput, low latency, minimal distortion, and high reliability due to this and other new features.

It should be noted that the availability of the 6 GHz spectrum was already introduced with the last evolutionary stage of Wi-Fi 6, the so-called Wi-Fi 6E. Even though not all countries allow for the available spectrum of the 6 GHz band, it represents a significant achievement of the Wi-Fi technology. Data transfer rates, capacity, interference, and latency have all been improved with this new spectrum.

Similar to the transition from fourth (4G) to fifth generation (5G) mobile technology, the introduction of the Wi-Fi 7 standard brings significant improvements over the previous technology. This is summarized in the graphical representation of Figure 1, demonstrating that Wi-Fi 7 provides significant enhancements in area traffic capacity, peak data rates, mobility, and spectrum efficiency.

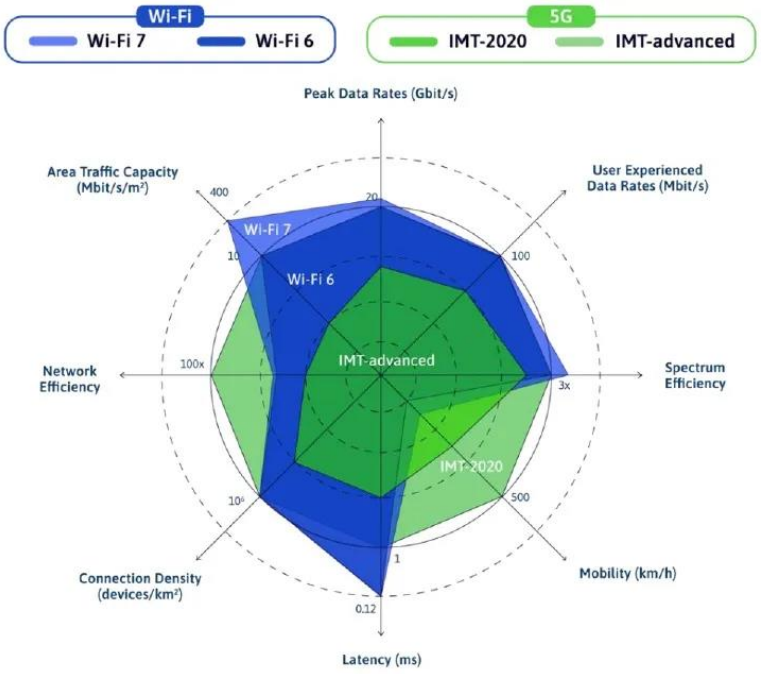

Wi-Fi 7 use cases

AR/VR/MR/XR

Extended reality (XR) comprises a wide range of applications with different levels of capability and complexity (Figure 2). Head-up display (HUD) shows a small image on glass in the user's head-mounted device (HMD) to display the status of one or more apps. The pictures, that can occupy the entire user's field-of-view, may be fixed or reflect the HMD's orientation. Image rendering can be done on a companion device and sent to the glass through P2P Wi-Fi to lessen its compute complexity.

VR is more immersive because the user is virtually represented in the application, including the HMD's stance and other features like hands, feet, etc., which are tracked by the built-in camera or other sensors. Training, industrial operations, and collaboration have almost endless applications. Immersion demands a lot of rendering compute, thus it's commonly offloaded to neighboring edge or computer resources. VR video rendering requires high throughput and short delay (latency).

The complexity and capabilities of AR and VR can be extended to mixed reality (MR), where HMD cameras gather live video for remote display/surveillance and contextual (object-recognition) applications. MR, the most complicated XR application, often uses edge computing for compute offload.

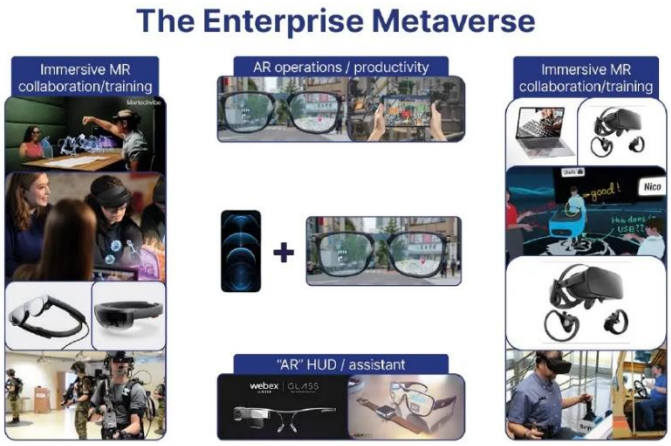

Gaming

Wi-Fi 7's unique features increase speeds and responsiveness for a more consistent and trustworthy online gaming experience. These include:

- Quicker download and upload speeds: Wi-Fi 7 reduces lag and improves the online gaming experience. Additionally, players will spend less time waiting to play because quicker transfer rates will allow them to receive game updates and fixes faster.
- Improved stability: Wi-Fi 7's multi-link operations reduce dropped connections, making the gaming more constant and stable. Client devices can connect to many bands simultaneously and, for better throughput, the device can utilize all bands or numerous links for redundancy. Competitive gamers who can't lose connectivity during a match may benefit from this.
- Expanded network capacity and lower latency: Wi-Fi 7 is called "Extremely High Throughput" because it adds 6 GHz channels to give gamers a clear signal.

IoT

The applications include:

- Autonomous Mobile Robots (AMR)
- AMR Video Fusion
- Safety Controls, such as Programmable Logic Controllers (PLCs)
- AR/VR/XR-based operations

Other potential use cases include video conferencing, wireless backhauls in enterprise deployments, service provider-managed homes, and Wi-Fi mesh architecture for future connected homes.

Conclusion

Higher speed, lower latency, increased reliability, and efficiency will improve connectivity with Wi-Fi 7. High throughput, low latency, and consistent performance will improve user experience for demanding applications including XR/AR/VR, online gaming, industrial IoT, and video conferencing. It will also support more devices in high-density installations and increase Wi-Fi in companies, industrial, and residential environments.

Following the Wi-Fi Alliance certification, WBA expects Wi-Fi 7 device enablement and network deployments to increase.

LOW VOLTAGE, SMALL FORM FACTOR GaN FETs: PRECISE CHARACTERIZATION

UTSAV CHATTERJEE, PRASENJIT MONDAL
3rd YEAR, ECE

Applications for 100-V (and lower) GaN FETs are extensive, ranging from reducing distortion in Class D audio amplifiers to enhancing the efficiency of synchronous rectifiers and motor drives. In addition to 48-V automotive and server applications, as well as USB-C, LiDAR, and LED illumination, these connectors are widely used.

However, the compact size and minimal packaging parasitics make it difficult to characterize these power devices dynamically. This article discusses the difficulties that GaN semiconductor manufacturers face when attempting to characterize these devices, as well as some novel technologies that help overcome these difficulties.

Wide-bandgap (WBG) devices have made significant strides in recent years to replace silicon-based power MOSFETs and IGBTs in a variety of power-related applications. Their fundamental properties allow for significant advancements in key power application areas. When comparing GaN to silicon, it is common knowledge that GaN's larger bandgap, higher electron mobility, and larger electric-field potential enable essential properties, such as lower losses (i.e., higher efficiency), faster switching, and a significantly smaller size (i.e., higher power density). In contrast to silicon, WBG devices have a much-limited history of use in a variety of power applications, particularly "high uptime" applications such as automotive.

JEDEC formed the JC-70 Committee in 2017 to develop needed new reliability, characterization, test methods and datasheet enhancements to appropriately characterize GaN and SiC WBG power devices. The existing Si-based standards were not sufficient to enable designers to determine the most appropriate WBG devices for their application. For example, on-resistance (RDS (on)), the main parameter characterizing conduction losses, is a dynamic phenomenon in GaN, based on the charge being trapped in the transistor structure (current collapse). JEP-173 was JC-70's first publication (issued in January 2019) to provide a standard for "dynamic on-resistance test method guidelines for GaN HEMT–based power-conversion devices."

Examples of low-voltage GaN FET applications

One application of the initial Class D audio amplifiers was sound systems for automobiles. The amplifier's lower power dissipation and superior efficiency (>90%), compared with Class A amplifiers, enabled "limited power" automobiles the ability to have multiple speakers and more sound (>100 W). However, the tradeoff for less power consumption was higher total harmonic distortion (THD), created by slower-switching power Si MOSFETs. GaN FETs with significantly faster switching speeds (up to 10×) and no reverse-recovery charge provide a superior linear response and significantly reduced THD.

In addition to automotive applications, you've probably noticed the recent boom in portable speakers. As well as advances in battery technology, this application is enabled by efficient, compact Class D audio amplifiers designed with GaN FETs. Good audio quality is provided because of the lower-distortion attributes of GaN, while the ability to run for extended times on batteries is possible because of GaN's high efficiency. There are many other portable consumer devices that can leverage the same attributes as portable speakers.

Automotive systems are moving toward higher-voltage operation (e.g., 48 V) as more electrical power needs develop for autonomous driving, including radar, cameras, ultrasonic sensors and LiDAR. These functions require uninterrupted, highly reliable power. As the 48-V bus emerges as one of the new higher-voltage power systems, efficiency is again the key with a limited power source (i.e., car battery). GaN technology enables better power density than silicon, minimizing additional weight, size and thermal management. GaN's higher-frequency switching and increased efficiency also reduce necessary passive component size (e.g., inductors), further minimizing the size of the power-converter design. DC/DC converters (12–48 V) made from these GaN FETs enable the standard 12-V power bus to supply power for these emerging automotive system requirements.

The motor drive (e.g., stepper motors, drones, etc.) is yet another large application for 100-V (and lower) GaN devices. Low losses often remove the need for heatsinks. GaN enables higher-frequency PWM signals and significantly reduces switching losses. Higher-frequency switching reduces/eliminates switch-node oscillations, which often require snubber circuits in Si-based designs.

The are many evolving applications primed to take advantage of GaN's superior performance compared with silicon. But the challenges to characterize these devices follow the themes described above: small size (power density) and higher efficiency.

Challenges characterizing low-voltage, small-form–factor GaN power devices

The first major challenge is the package size. Many of the 100-V (and less) GaN FET packages are ball-grid arrays (BGA) ranging from a few millimeters in the X and Y dimensions to sub-millimeters in the X and Y dimensions. These packages have from a 2 × 2 matrix of solder balls to a 5 × 15 matrix of solder balls. Figure 1 shows an example of an EPC2045, 100-V, 16-A GaN e-HEMT device with a specified RDS (on) of 7 mΩ.

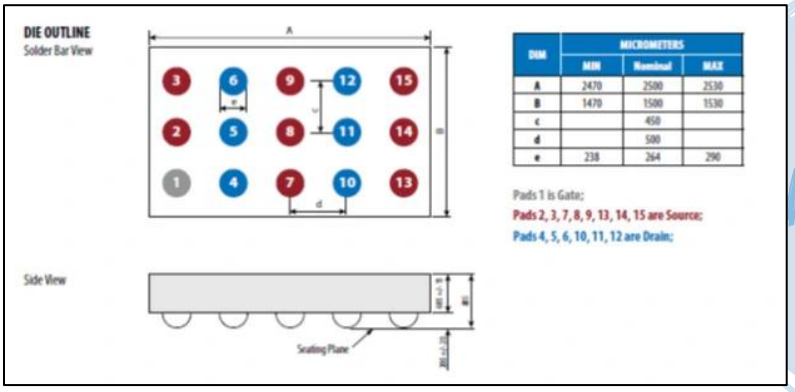

DIM	MICROMETERS		
	MIN	Nominal	MAX
A	2470	2500	2530
B	1470	1500	1530
c		450	
d		500	
e	238	264	290

HIGH VOLTAGE ELECTROPORATION WITH PRECISION POWER SOLUTIONS

ANKAN SARKAR, GOURAV KUMAR
1st YEAR, ECE

Pulsed electric field, also known as electroporation, is an exciting advancement in electrosurgery and life sciences that enables the development of numerous novel treatments. As a result, this technique is gaining popularity. Pulsed field ablation (PFA) research and development is of particular interest because the ultra-short pulses increase therapeutic effects while minimizing thermal issues.

However, effective system designers must be capable of accurately delivering high-voltage (HV) electrical energy. As researchers continue to refine their methods, these systems must accommodate a variety of parameters without sacrificing control precision.

This article from Advanced Energy examines the developments and challenges in this sector and their implications for the design of power systems. The article will also examine some of the essential components of such a system.

Electroporation is a technique in which HV (typically thousands of volts per centimeter) is administered to cells to increase membrane permeability. Reversible and irreversible forms of electroporation exist.

Electroporation that employs a low-intensity electric field that does not exceed the threshold of the target tissue is described as reversible. This allows chemicals, medications, and DNA to penetrate the cell. Electrochemotherapy has primary applications in gene transfer and electrochemotherapy.

Irreversible electroporation (IRE) is the creation of permanent pores when the electrical field exceeds the target tissue's threshold. These permanent pores lead to cellular homeostasis disruption, culminating in cell death. Primary applications of IRE include cardiac ablation and tumor ablation.

From a technical perspective, the difference between the two electroporation types is simply a function of the electrical field strength and the duration for which the field is applied.

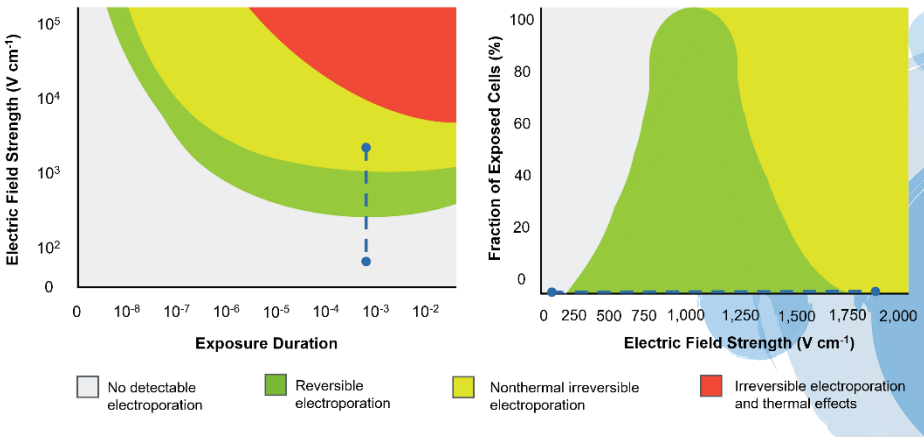

As a technique for delivering electroporation, PFA is a non-thermal energy modality that has been utilized for solid organ tumor ablation for some time. More recently, investigators have demonstrated a unique safety profile and ablative efficacy related to its ability to selectively target cardiomyocytes while sparing collateral damage to the connective tissue structure. This has driven significant research into different pulse trains to determine the most effective approach for various use cases.

Established PFA approaches apply between 80 and 120 unipolar pulses, with a pulse duration of 50 to 100 ms and an electric field that exceeds 1,000 V/cm. While it can be effective, this typical IRE protocol may evoke muscle contraction during the procedure, leading to pain for the patient and causing displacement of the electrode needles.

Recently, a new type of IRE technique called high-frequency IRE (H-FIRE) has emerged. H-FIRE uses a set of bipolar pulse bursts consisting of individual pulses with durations from 0.5 to 10 ms, grouped into a burst of up to 100 ms.

As a specific example, there are multiple documented studies for the application of IRE to liver tumors, with the earliest dating back to 2011. The tumors ranged in size from 2 mm to 100 mm, although there was a high degree of commonality between the electrical parameters of the IRE treatment. The applied voltage was always in the range of 1.5–3 kV/cm, with a duration of 70–100 μs, and the best results were obtained using plate electrodes to deliver 80 pulses of 100 ms at 0.3 Hz, with an electrical field magnitude of 2.5 kV/cm across the tumor.

The PFA challenge for power designers

The primary challenge of power solution design for PFA systems is the need to deliver high-energy HV pulses reliably and repeatably. For life-science applications, typically a power system in the 2- to 300-W region is all that is required. For surgical applications like PFA, individual pulses can be up to 20 kW, with an average power for the system in the kilowatt region.

As research continues, the required waveform evolves, which can increase the challenge for power design. The unipolar pulses of early IRE have evolved into bipolar pulses, which may be symmetric or asymmetric.

The voltage required is typically in the 1-kV to 3-kV range, with some applications requiring up to 5 kV with currents up to 65 A. Pulse widths are typically in the range of 100 ns to 100 μs, with burst-mode frequencies up to 5 MHz. The associated slew rates for the pulse are both significant and challenging.